Available online at www.sciencedirect.com
ScienceDirect
Advances in Space Research 41 (2008) 1619–1629
ADVANCES IN SPACE RESEARCH (a COSPAR publication)
www.elsevier.com/locate/asr

The plasma sheet and boundary layers under northward IMF: A multi-point and multi-instrument perspective

M.G.G.T. Taylor [a,b,*], B. Lavraud [c], C.P. Escoubet [a], S.E. Milan [d], K. Nykyri [e,f], M.W. Dunlop [e,g], J.A. Davies [g], R.H.W. Friedel [c], H. Frey [h], Y.V. Bogdanova [b], A. Åsnes [a], H. Laakso [a], P. Trávnícek [i,j], A. Masson [a], H. Opgenoorth [a], C. Vallat [a], A.N. Fazakerley [b], A.D. Lahiff [b], C.J. Owen [b], F. Pitout [k,l], Z. Pu [m], C. Shen [n], Q.G. Zong [o], H. Rème [p], J. Scudder [q], T.L. Zhang [r]

[a] *ESA/ESTEC, Keplerlaan 1, 2200 AG Noordwijk, The Netherlands*
[b] *Mullard Space Science Laboratory, University College London, Dorking, Surrey RH5 6NT, UK*
[c] *Space Science and Applications, Los Alamos National Laboratory, Los Alamos, New Mexico, USA*
[d] *Department of Physics and Astronomy, University of Leicester, Leicester LE1 7RH, UK*
[e] *The Blackett Laboratory, Imperial College London, London SW7 2AZ, UK*
[f] *Embry-Riddle Aeronautical University, FL, USA*
[g] *Space Science and Technology Department, Rutherford Appleton Laboratory, Oxfordshire, UK*
[h] *Space Science Laboratory, University of California, Berkley, CA 94720, USA*
[i] *Astronomical Institute, Academy of Sciences of the Czech Republic, Czech Republic*
[j] *Institute of Atmospheric Physics, Academy of Sciences of the Czech Republic, Czech Republic*
[k] *Max-Planck-Institut für Aeronomie, D-37191 Katlenburg-Lindau, Germany*
[l] *Laboratoire de Planetologie de Grenoble, BP 53, 38041 Grenoble Cedex 9, France*
[m] *School of Earth and Space Sciences, Peking University, Beijing 100871, China*
[n] *Centre for Space Science and Applied Research, Chinese Academy of Sciences, Beijing 100080, China*
[o] *Center for Atmospheric Research, University of Massachusetts, Lowell, USA*
[p] *Centre d'Etude Spatiale des Rayonnements, Toulouse, Cedex 4, France*
[q] *Department of Physics and Astronomy, University of Iowa, IA 52242, USA*
[r] *IWF, Space Research Institute, Austrian Academy of Sciences, Graz, Austria*

Received 28 November 2006; received in revised form 26 September 2007; accepted 12 October 2007

Abstract

During conditions of northward interplanetary magnetic field (IMF), the near-tail plasma sheet is known to become denser and cooler, and is described as the cold-dense plasma sheet (CDPS). While its source is likely the solar wind, the prominent penetration mechanisms are less clear. The two main candidates are solar wind direct capture via double high-latitude reconnection on the dayside and Kelvin–Helmholtz/diffusive processes at the flank magnetopause. This paper presents a case study on the formation of the CDPS utilizing a wide variety of space- and ground-based observations, but primarily from the Double Star and Polar spacecraft on December 5th, 2004. The pertinent observations can be summarized as follows: TC-1 observes quasi-periodic (~2 min period) cold-dense boundary layer (compared to a hot-tenuous plasma sheet) signatures interspersed with magnetosheath plasma at the dusk flank magnetopause near the dawn-dusk terminator. Analysis of this region suggests the boundary to be Kelvin–Helmholtz unstable and that plasma transport is ongoing across the boundary. At the same time, IMAGE spacecraft and ground based SuperDARN measurements provide evidence of high-latitude reconnection in both hemispheres. The Polar spacecraft, located in the southern hemisphere afternoon sector, sunward of TC-1, observes a persistent boundary layer with no obvious signature of boundary waves. The plasma is of a similar appearance to that observed by TC-1 inside the boundary layer further down the dusk flank, and by TC-2 in the near-Earth magnetotail. We present com-

* Corresponding author. Address: ESA/ESTEC, Keplerlaan 1, 2200 AG Noordwijk, The Netherlands.
E-mail address: mtaylor@rssd.esa.int (M.G.G.T. Taylor).

0273-1177/$34.00 © 2007 COSPAR. Published by Elsevier Ltd. All rights reserved.
doi:10.1016/j.asr.2007.10.013

parisons of electron phase space distributions between the spacecraft. Although the dayside boundary layer at Polar is most likely formed via double high-altitude reconnection, and is somewhat comparable to the flank boundary layer at Double Star, some differences argue in favour of additional transport that augment solar wind plasma entry into the tail regions.
© 2007 COSPAR. Published by Elsevier Ltd. All rights reserved.

Keywords: Plasma sheet; Magnetopshere; Cold dense plasma sheet; Cluster; Double star

1. Introduction

The plasma sheet is a particularly interesting region of the magnetosphere as it is the main source of plasma to the inner magnetosphere. Yet, the predominance of its source populations (solar wind and ionosphere) as a function of external conditions and, in general, its formation mechanisms are poorly understood. The magnetosphere is most active under southward interplanetary magnetic field (IMF). Solar wind is thought to gain access to the magnetosphere via reconnection at the dayside magnetopause, supplying the mantle/lobe region and in turn the plasma sheet via reconnection in the distant magnetotail (Dungey, 1961). With enhanced activity, the density and temperature of the plasma sheet tend to increase (Wing and Newell, 1998). Under predominantly northward IMF, reconnection typically occurs at high latitudes (Gosling et al., 1990; Kessell et al., 1996; Lavraud et al., 2002) resulting in much quieter geomagnetic conditions, although low latitude reconnection, equatorward of the cusps, has also been observed during northward IMF (Chandler et al., 1999; Trattner et al., 2004). During prolonged periods of northward IMF, the characteristics of the plasma sheet are markedly different from the same region under southward IMF. The plasma sheet is substantially cooler and denser (Teresawa et al., 1997); it is termed the cold-dense plasma sheet (CDPS). Previous studies (e.g., Teresawa et al., 1997; Øieroset et al., 2003) have suggested several transfer mechanisms to supply the plasma sheet with solar wind plasma, with the prime candidates being (1) transfer across the flank magnetopause via the Kelvin–Helmholtz (KH) instability (Fujimoto and Teresawa, 1995; Hasegawa et al., 2004) and (2) reconnection in both hemispheres, poleward of the cusps (Song and Russell, 1992; Ogino et al., 1994; Fedder and Lyon, 1995; Raeder et al., 1995, 1997). Fig. 1 illustrates those two mechanisms. More recent studies have been able to identify transport processes related to CDPS formation. Utilising Cluster observations, Hasegawa et al. (2004) provided evidence for KH transport at the flank magnetopause. Øieroset et al. (2005), Lavraud et al. (2005, 2006), Li et al. (2005) and Imber et al. (2006) used spacecraft, MHD simulation, and/or ground-based data to identify the occurrence of high-latitude reconnection in both hemispheres, thus potentially leading to magnetopause boundary layer and CDPS formation.

In this paper, we present multi-point, multi-spacecraft observations of the formation of the CDPS during a period of sustained northward IMF during the passage of a Coronal Mass Ejection (CME) at Earth. During the event, there are observations of simultaneous lobe reconnection in both hemispheres, accompanied by a persistent dayside boundary layer of similar properties to the nightside CDPS. In addition, KH waves are observed on the dusk flank magnetopause, along with signatures that would support plasma transport across the boundary. Spectral comparisons of populations from these various regions suggest that although the dayside boundary layer (most likely formed by double lobe reconnection) has comparable plasma properties to that of the CDPS, the final content of the CDPS is most likely augmented by flank activity and transport.

2. Overview of 5th December 2004

On December 3rd, 2004, instruments on the Solar and Heliospheric Observatory (SOHO) (Domingo et al., 1995) spacecraft observed a halo CME. The passage of the CME at the ACE spacecraft (e.g., Stone et al., 1998) was characterized by a jump in magnetic field, plasma density and velocity at ~06:55 UT on December 5th, 2004. The ACE magnetic field (Smith et al., 1998), plasma speed and density (McComas et al., 1998) observations are shown in Figs. 2a–c from 07:00 to 23:00 UT, shifted by a lag of 55 min, (calculated from the bulk speed and upstream distance from the Earth of ACE just after it observed the CME). Following the initial CME impact, the solar wind speed gradually decreased from 450 to 400 km/s accompanied by a decrease in the density from ~80 to 20 cm^{-3}. The IMF remained predominantly northward, with a clock angle ($\tan \theta_{IMF} = B_Y/B_Z$) between −45 and 0 degrees, for an extended period from 09:00 to 17:00 UT. Fig. 2d–h show electron density, temperature and energy spectrogram measurements from the TC-1 PEACE (Fazakerley et al., 2005), TC-2 PEACE and Polar Hydra (Scudder et al., 1995) instruments. The corresponding spacecraft positions are shown in Fig. 3.

At the beginning of the period, TC-1 is located in the flank magnetosphere, in a characteristic hot and tenuous plasma sheet (HTPS). The impact of the CME at ~07:46 UT, compresses the magnetosphere and TC-1 enters the magnetosheath, where it remains until ~16:45 UT. TC-1 then encounters the magnetopause, characterised by quasi-periodic bursts of heated magnetosheath-like plasma (i.e., typical of magnetopause boundary layers and cold, dense plasma sheet; CDPS) interspersed with the typical, colder magnetosheath plasma. After ~18:30 UT, TC-1 enters a more persistent boundary layer- or CDPS-type population with electron temperatures of order 1–2 MK, which gradually rise, up to the end of the period. At the beginning of the period dis-

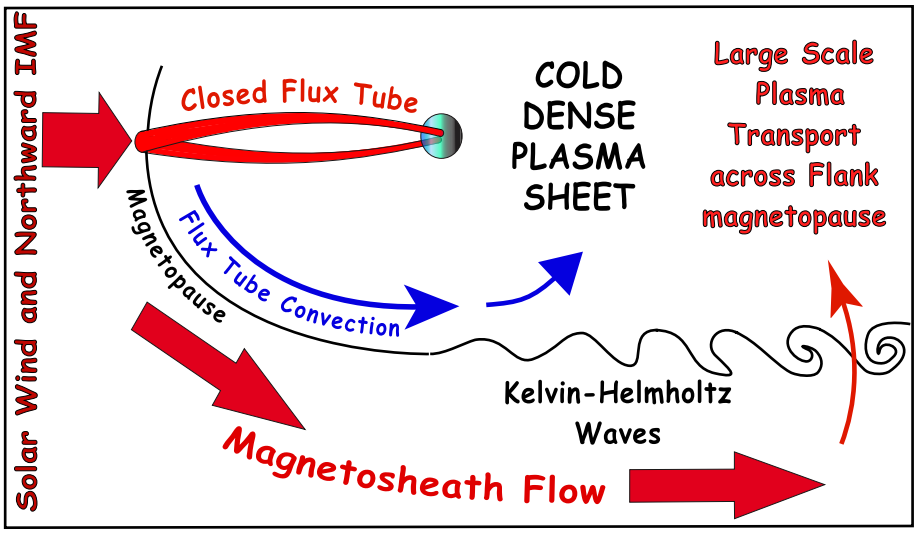

Fig. 1. Cartoon of magnetosphere in x–y plane, highlighting the CDPS source primary candidates: Double Lobe reconnection and Flank wave activity and transport.

played in Fig. 2, Polar is near perigee and swiftly crosses numerous near-Earth regions (e.g., radiation belts). It then moves into the magnetosheath around 12:30 UT, where it remains until ~16:00 UT apart from ~6 excursions across the magnetopause. Comparing TC-1 and Polar measurements in the magnetosheath, there is around a factor 2–4 difference in density and ~2 in temperature, most likely due to instrumental differences (i.e., energy ranges and sensitivities), which gives us a reference point for later comparisons. At 16:00 UT, Polar passes the magnetopause and observes a boundary layer until 21:00 UT after which there is no Hydra data. During the period 16:00–21:00 UT Polar passes through apogee, with radial distances within the envelope ~9.4–8.5 R_E, while the density ~1–2 #/cc and temperature ~1–2 MK remain reasonably stable and typical of boundary layer plasma. We note the similarity of this population to that observed by TC-1 between 18:30 and 20:30 UT. Finally, for TC-2, at ~09:00 UT the spacecraft is in the outer radiation belts, after which it enters the dusk flank hot-tenuous plasma sheet (HTPS) (energies ~keV's) at higher latitudes. We note that the gaps in the TC-2 moments are due to instrument operation and periods when the spacecraft potential could not be reliably determined. A gradual decrease in electron temperature is observed until ~14:00 UT, when the spacecraft records a much denser population (CDPS) with 1–2 MK temperature, comparable to the plasma observed at TC-1 between 18:00 and 21:00 UT and the boundary layer population at Polar between 16:00 and 21:00 UT. This population at TC-2 is persistent, although interspersed with some brief plasma mantle/lobe encounters, up to ~18:00 UT when the instrument is powered down. Just after 20:00 UT the instrument is powered on just outside the radiation belts, which is followed by a rather rarefied mantle/lobe-like encounter. Unlike the previous orbit, there is little evidence of tenuous plasma sheet populations, although there are remnants of the 1–2 MK CDPS population, albeit at a slightly lower density.

3. CDPS formation

3.1. Dayside observations

Fig. 4a shows data from the SuperDARN radars (Greenwald et al., 1995) in the form of a convection map (e.g., Runohoniemi and Baker, 1998), between 15:04 and 15:06 UT. Fig. 4b shows data from the IMAGE FUV instrument (Mende et al., 2000) on a projection of the Earth's southern hemisphere from 15:05:05 UT. From the SuperDARN data there is clear sunward convection in the ~12 MLT sector, which is typically associated with high-latitude reconnection (Milan et al., 2000). Such convection is prevalent throughout the time period 12:50–15:30 UT, thereafter the data becomes patchier and the convection pattern becomes less defined, although there are intervals of sunward flow evident up to 18:00 UT. In Fig. 4b, between 13 and 14 MLT and at latitudes above −80°, IMAGE FUV data shows clear evidence of an auroral spot, poleward of the sub-solar oval, also consistent with high-latitude reconnection (Milan et al., 2000; Frey et al., 2002). This spot is persistent, with varying intensities, from ~12:00 to 17:00 UT. The data from SuperDARN are from the northern hemisphere while those from IMAGE are from the southern hemisphere, thus providing evidence that high-latitude reconnection is ongoing in both hemispheres at the same time.

In Fig. 5, we show Polar data around the time period of the magnetopause crossing. At around 15:56 UT Polar crosses the magnetopause and enters a low-latitude boundary layer (LLBL) characterized by a rotation in the magnetic field (Russell et al., 1995), an increase in electron temperature, and a reduction in flow velocity (derived from

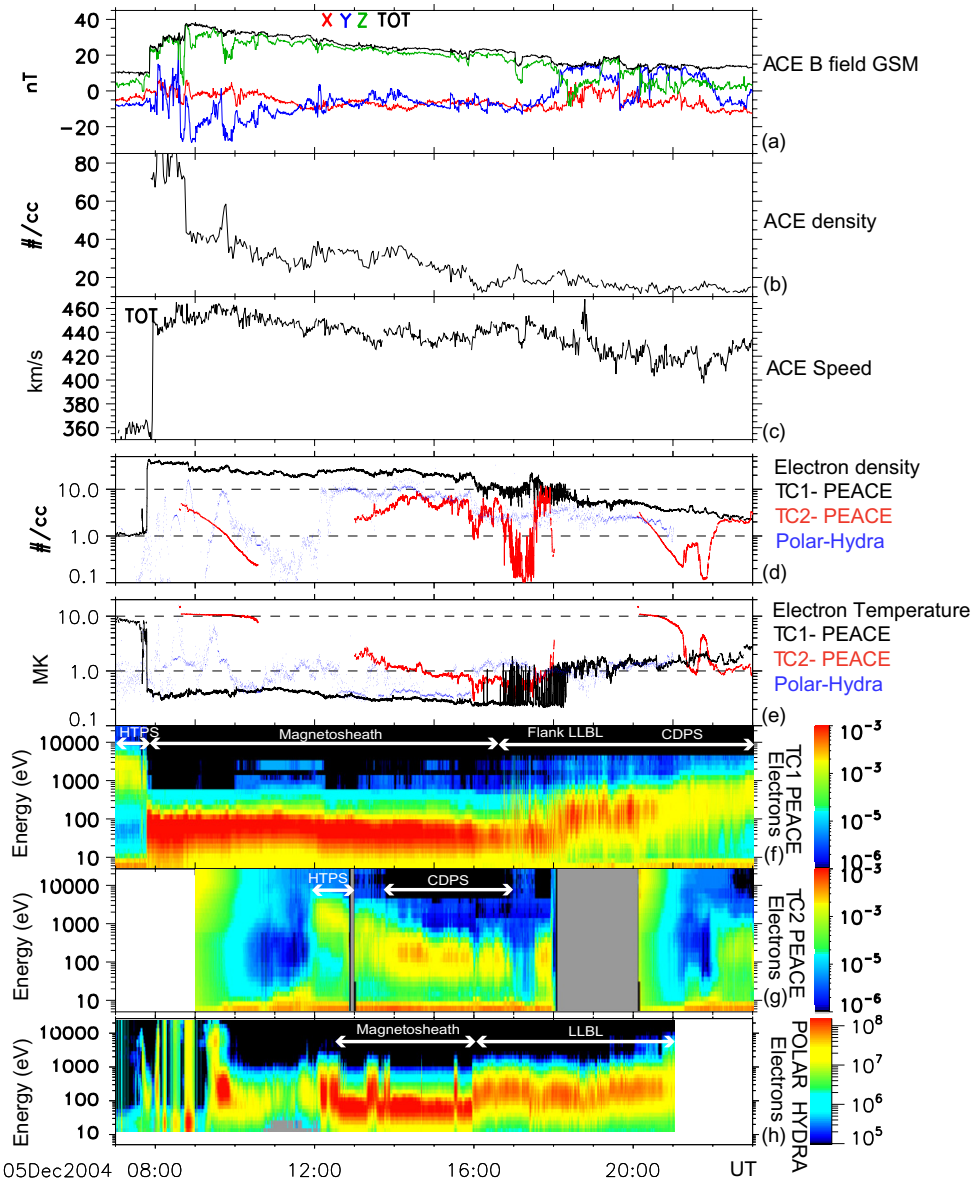

Fig. 2. ACE (shifted by 60 min), TC-1, Polar and TC-2 plasma and magnetic field observations from 5th December 2004, 07:00–23:00 UT; (a) ACE IMF GSM components; (b) ACE solar wind density; (c) ACE solar wind speed; (d) TC-1, TC-2 and Hydra electron density; (e) TC-1, TC-2 and Hydra electron temperature; (f) TC-1 electron spectrogram; (g) TC-2 electron spectrogram; (h) Hydra electron spectrogram. CME impact of magnetosphere is observed at ~07:46 UT. Magnetospheric regions are marked in panels (f–h).

electric (Harvey et al., 1995) and magnetic field measurements). The magnetopause crossing is also accompanied by an increase in the electron temperature ratio ($T_{\text{Parallel}}/T_{\text{Perpendicular}}$). The formation of the LLBL has been discussed in numerous studies, primarily via diffusive/viscous (e.g., Scholer and Treumann, 1997; Phan et al., 1997; Johnson et al., 2001) or reconnection (e.g., Onsager et al., 2001) processes. Under the sole action of diffusive entry, Treumann et al. (1995) suggested that boundary layers could only be formed up to thicknesses of ~0.5 R_E. Such transport could be enhanced by Kelvin–Helmholtz (KH) waves, which have been observed at the dayside magnetopause upstream of the terminator (Hasegawa et al., 2006). In the current case, we estimate the radial extent of the boundary layer, based on the position of the spacecraft at the magnetopause crossing and the end of the data interval, to be ~0.9 R_E (although the orientation of the Polar orbit is such that the spacecraft may be skimming the magnetopause, and hence moving parallel to, rather than perpendicular to the boundary). The magnetopause crossing is rather rapid, such that characterization of the local magnetopause boundary is difficult. The crossing is identified by significant shear in the magnetic field (most notable in the y component) which along with the electron temperature and density in the boundary layer, show no strong signs of wave activity, although the ExB velocity shows periodic enhancements in the $-x$ direction. Considering the northward IMF conditions during this time, the

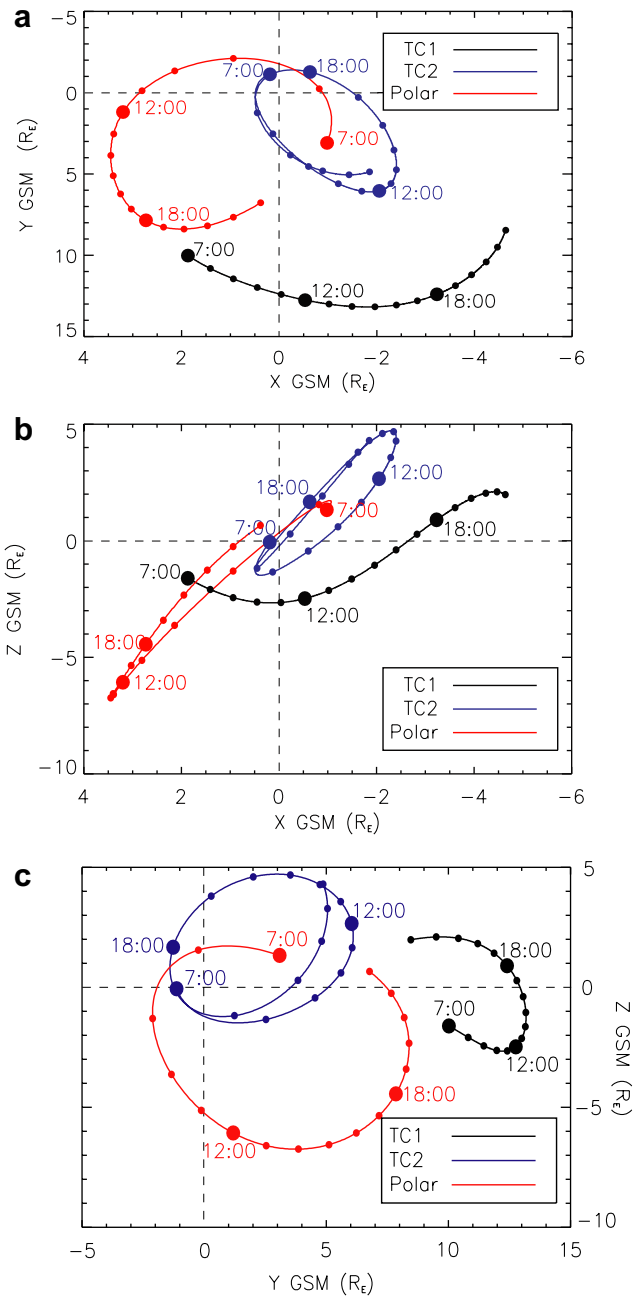

Fig. 3. TC-1, TC-2 and Polar orbit plot in GSM from 07:00 to 23:00 UT, 5th December 2004.

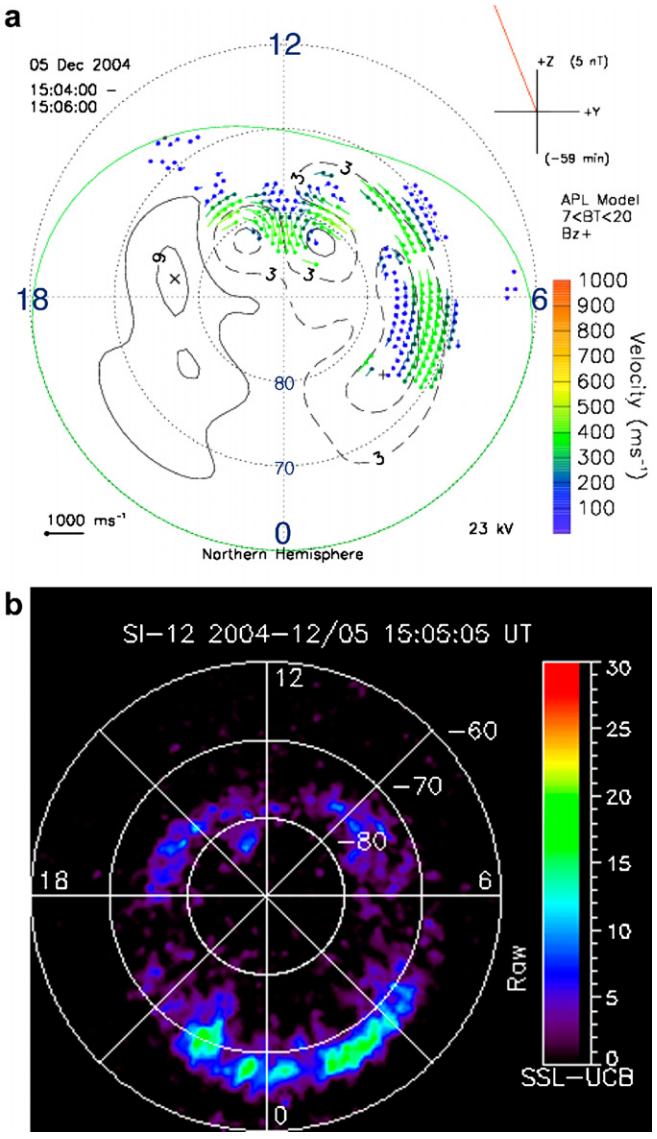

Fig. 4. (a) SuperDARN convection map showing sunward convection in the 11–13 MLT sector associated with lobe reconnection in the northern hemisphere. (b) IMAGE FUV data showing a clear spot poleward of the sub-solar oval, consistent with a southern hemisphere lobe reconnection site.

observation of heated electrons (predominantly along the magnetic field) in the boundary layer, and the evidence of reconnection ongoing in both lobe simultaneously lead us to suggest that it is most likely that the LLBL observed at Polar has been formed by the capture of magnetosheath field lines at both lobes (e.g., Onsager et al., 2001; Lavraud et al., 2005, 2006; Li et al., 2005; Imber et al., 2006). We note that we cannot totally rule out diffusive/KHI processes in forming the LLBL in this case, but there is more evidence related to the mechanism of double lobe reconnection.

3.2. Flank activity

Fig. 6 shows TC-1 magnetic field (FGM, Carr et al., 2005), ion (HIA, Rème et al., 2005) and electron (PEACE) data from 16:15 to 19:30 UT, as TC-1 moves from the magnetosheath into the magnetosphere. The crossing shows the quasi-periodic (~2 min) appearance of boundary layer plasma with higher temperature, lower density and reduced magnetic field magnitude compared to the adjacent magnetosheath. During the period when TC-1 observes this boundary, the Cluster spacecraft are located in the southern hemisphere afternoon sector of the magnetosheath. Cluster data does not show any similar perturbations there, suggesting the TC-1 observations are locally driven. These periodic signatures are similar to previous flank study

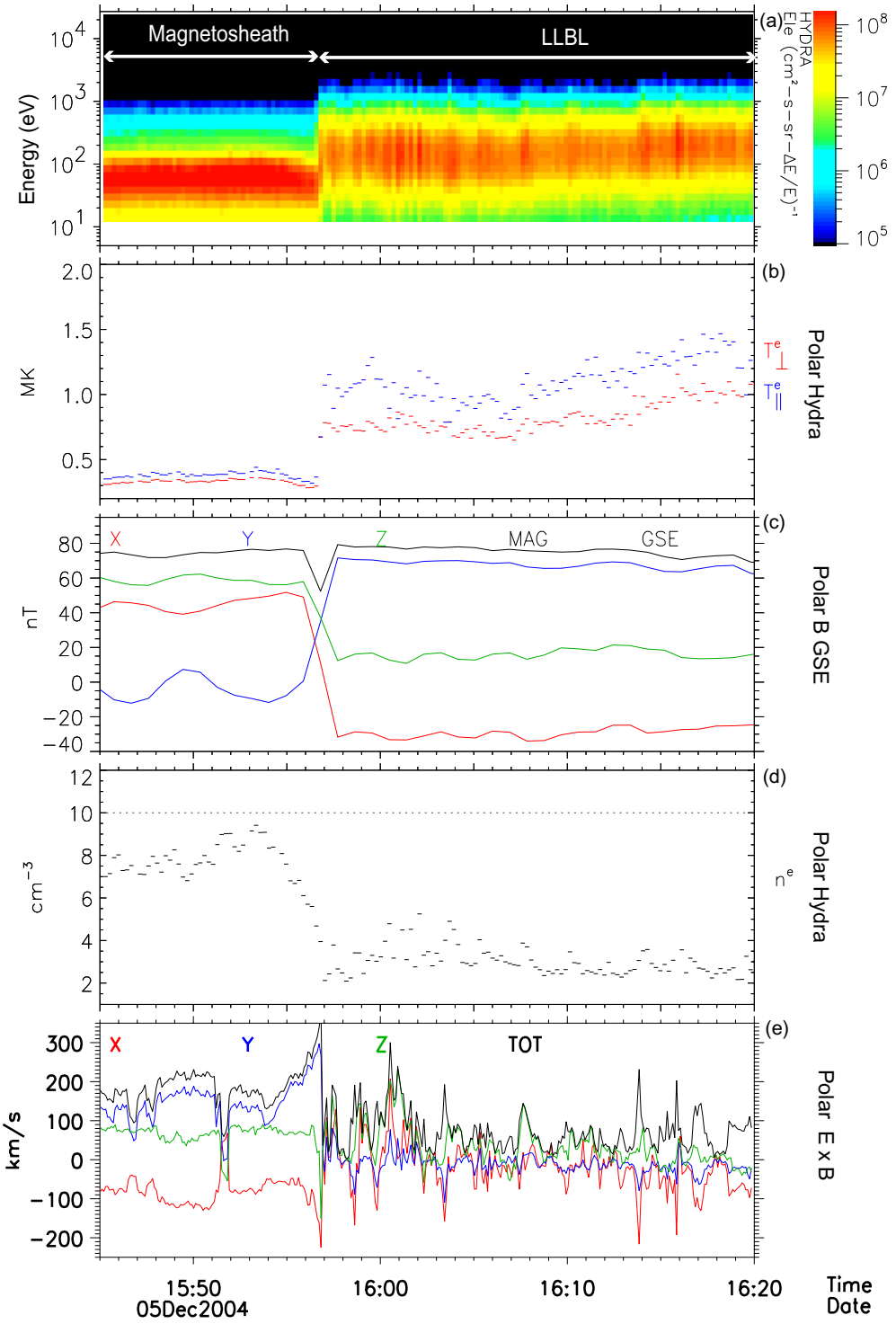

Fig. 5. Detail of Polar magnetopause crossing. (a) Hydra electron spectrogram; (b) Polar electron temperature; (c) Polar Magnetic Field GSE; (d) Polar electron density; (e) Polar ExB velocity.

reports of KH surface waves (e.g., Fairfield et al., 2000; Hasegawa et al., 2004). We carried out a 2.5 dimensional, high-resolution local MHD simulation (e.g., Otto and Fairfield, 2000; Nykyri, 2002) using ion and magnetic field values measured by TC-1 on the sheath and boundary layer side of the magnetopause. Fig. 7 shows the simulation results after 230 s, with magnetic field (arrows) and z-component of the current density, j_Z, (color coded) plotted in the left hand panel and velocity (arrows) and density (color coded) in the right hand panel. The plot is normalized to a number density 15 cm^{-3}, magnetic field 45 nT and velocity 253 km/s, with the k vector of the wave in the shear flow plane. The black lines are the magnetic field lines projected on the shear flow plane, generated by

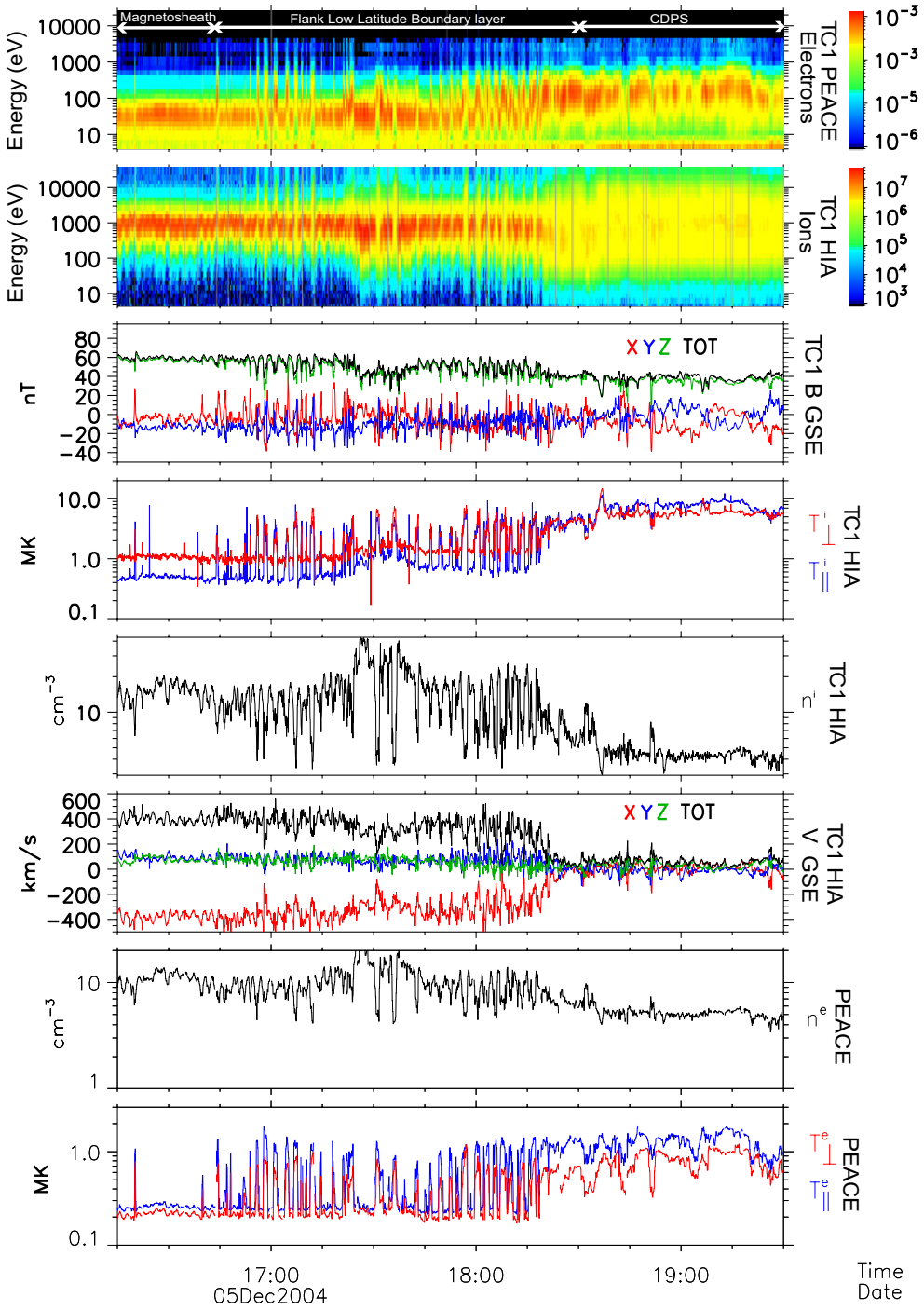

Fig. 6. Detail of TC-1 magnetopause crossing. (a) TC-1 electron spectrogram (ergs/s cm^2 sr eV); (b) TC-1 Ion spectrogram (keV/s cm^2 sr keV); (c) TC-1 FGM B field GSE; (d) TC-1 ion temperature;(e) TC-1 ion density; (f) TC-1 ion velocity; (g) TC-1 electron density; (h) TC-1 electron temperature.

projecting the observed magnetospheric and magnetosheath magnetic field lines along the magnetosheath velocity direction. In this configuration, the magnetic field is mostly perpendicular to the shear flow plane, hence satisfying the KH instability onset conditions. Note in Fig. 7a that the smaller magnetic field vectors on the magnetosheath side results from the projection discussed above.

In Fig. 7, we observe rolled-up KH wave and at $[x, y] \sim [10,-1]$ magnetic reconnection within the vortex leads to the formation of a detached high density filament of magnetosheath origin, in a similar manner as discussed in (Nykyri and Otto, 2001). Such transport of plasma via non-linear KH waves has been the subject of recent studies (Nykyri et al., 2006; Hasegawa et al., 2006). In particular, Hasegawa et al. (2006) compared observations with a three dimensional MHD simulation (Takagi et al., 2006) for the event of Hasegawa et al. (2004) and presented a single spacecraft method to detect rolled-up vortex structures at

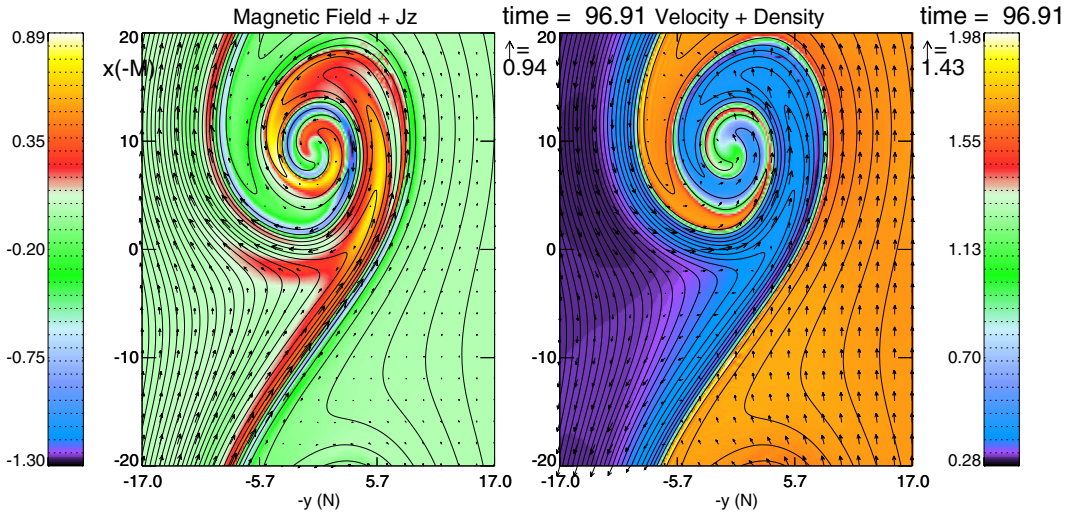

Fig. 7. MHD simulation result of the boundary observed at TC-1, input parameters from in situ ion and magnetic field measurements. The magnetic field (arrows) and j_Z (color) are plotted on the left hand side and the velocity (arrows) and density (color) on the right hand side. The black lines are magnetic field lines.

the flank magnetopause. By comparing the velocity and density across the magnetopause in simulation and spacecraft data, Hasegawa et al. (2006) showed that rolled-up vortex structures are characterized by lower density (typical of the boundary layer plasma involved in the KH process) regions which tailward speeds are larger than that of the magnetosheath itself. In Fig. 8, we show a scatter plot of the TC-1-HIA V_x component and density for the time period 16:30–18:30 UT, where we assume the x GSM direction to be tangential to the magnetopause. Magnetosheath plasma characteristically has high speed and high density (right part of Fig. 8) while magnetospheric/boundary layer plasma typically has lower density and speed (top-left part). However, the significant number of higher speed, low-density points in the lower left part of Fig. 8 suggests that rolled-up vortices are developed at the boundary, and as such, that the KH instability may facilitate the transport of plasma (Hasegawa et al., 2006). This transport (suggested by the existence high-speed, low density points) may thus be enabled as a result of the occurrence of magnetic reconnection within rolled-up vortices, compatible with the simulation results presented above and previous studies (e.g., Nykyri et al., 2006; Nakamura et al., 2006).

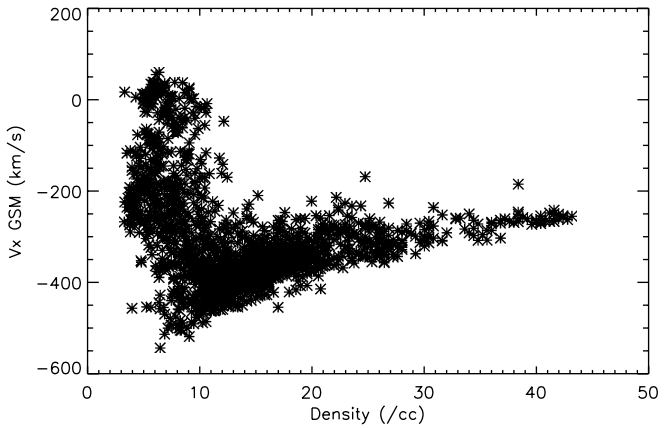

Fig. 8. TC-1 HIA V_X component of velocity (GSM) in km/s and density in #/cc for the time period 16:30–18:30 UT. The significant number of point in the lower left part of the plot suggests plasma transport is ongoing across the magnetopause (Takagi et al., 2006; Hasegawa et al., 2006).

4. Discussion

The observations presented above provide a multi-point perspective of the impact of a sustained northward IMF interval (owing to the passage of a CME) on Earth's magnetosphere. Of particular interest is the evolution of the near-Earth magnetotail and flank regions from hot and tenuous to cold and dense. We note that the CDPS-like material was initially observed between 13 and 14 UT by TC-2 at ~(−2, 6, 2) in GSM, approximately 5–6 h after the impact of the CME as determined by the magnetospheric compression observed at TC-1 (Fig. 2). In addition, LANL geosynchronous data from two spacecraft located in the midnight region (not shown) show the appearance of CDPS-like material about 4 h after the CME impact. This can be compared to the 3 h timescale reported by Øieroset et al. (2003).

Both TC-1 and TC-2, separated by several R_E, make observations of both the hot-tenuous and cold-dense populations. This is illustrated in Fig. 9a, where we have taken representative cuts of the electron phase space density (PSD) distributions averaged over 20 minutes, centered on the time indicated in the legend. The solid lines represent the hot-tenuous plasma sheet observations (07:15 UT at TC-1 (black) and 12:15 UT at TC-2 (blue)), and show good agreement. Within 3 h, TC-2 has moved to higher latitudes and begins to observe CDPS-like material. Comparing this population at 15:30 UT at TC-2 with the distribution observed by TC-1 at 19:30 UT (dotted lines

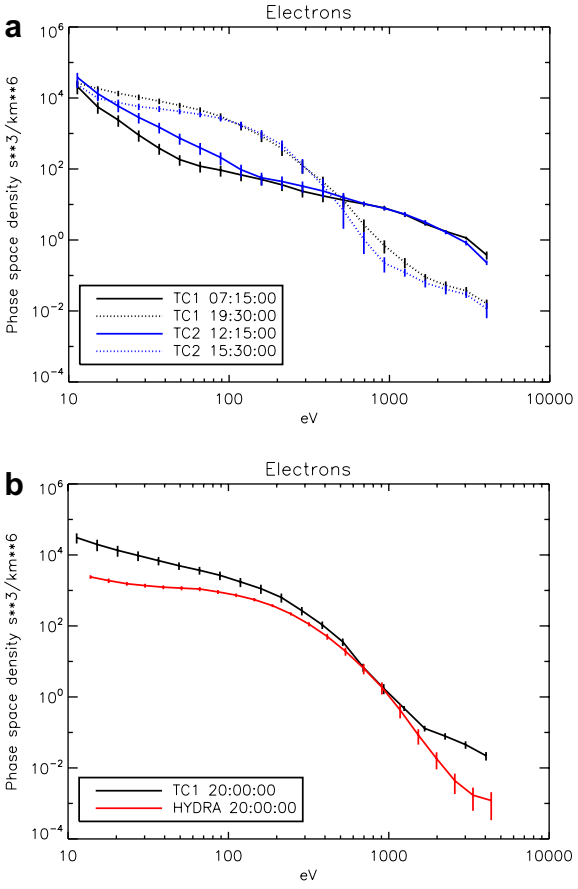

Fig. 9. Phase space density distributions, averaged over time and look direction over 20 min centered on the times indicated. (a) TC-1 and TC-2 PEACE electron data comparing spacecraft and contrasting HTPS and CDPS regions. (b) electron data from the boundary layer at Polar and the CDPS at TC-1.

in Fig. 9a), we find the CDPS PSD distributions to be quite similar. By mapping field lines (using the Tsyganenko 96 magnetic field model (Tsyganenko and Stern, 1996) with appropriate input conditions) from TC-2 at 15:30 UT to the equatorial plane, we find that TC-2 is magnetically connected to the dusk flank boundary layer, approximately at the location that TC-1 later crosses the magnetopause. As time (and hence TC-2 latitude) increase, TC-2 maps further down the flank.

In Fig. 9b, we present a similar comparison of electron distributions, on this occasion from TC-1 (black) and Polar (red). As discussed previously, the boundary layer observed by Polar was most likely formed by double high-latitude reconnection. Comparing the Polar observations to those at TC-1, we note that the boundary layer at TC-1 shows larger phase space densities in the entire sub-100 eV range. Although inter-calibration issues between the instruments exist, because (1) there is an order of magnitude difference in PSD at low energies while not at higher energies, and (2) the boundary layers at each spacecraft are observed on the same side of the magnetosphere, at the same time and close to the magnetopause, these PSD distributions suggest that if plasma were moving from Polar to TC-1 (i.e., blue arrow trajectory in Fig. 1) an additional source of plasma would be needed, in particular at low, magnetosheath-type energies. One may also come to a similar conclusion by examining the densities at Polar and TC-1 in Fig. 2. If the plasma is simply convected from Polar to TC-1 in an expanding flux tube, one should expect the density at TC-1 to be less than Polar. As pointed out in Section 2, there is a factor of 2–4 difference in the values between Polar and TC-1 in the magnetosheath (due to differences in energy range and instrument response). Comparing the densities of the boundary layer observed at both spacecraft (16:30 UT at Polar and 21:00 UT at TC-1), a similar factor remains, although the magnetic field at TC-1 is at least half that observed at Polar, suggesting that the plasma at TC-1 is not simply convected from Polar, but its density is enhanced by an additional source.

We envisage that the KH instability is responsible for this additional PSD increase at TC-1 and therefore that additional plasma penetration results from this process at the TC-1 location. Since TC-1 measurements in the flank boundary layer are very similar to TC-2 observations mapped to the boundary at an earlier time, it is possible that the flank boundary layer existed from at least ~14:00 UT. Finally, we note the persistent existence of the CDPS population after the period of relatively strong northward IMF (>18:00 UT). After this time evidence of lobe reconnection in the IMAGE and SuperDARN data is much reduced, while the boundary layer at TC-1 endures, suggesting continuation of plasma transfer. In addition, during this period there is little magnetospheric activity, such that one may expect that under weak driving conditions, the CDPS may remain for longer before being replaced by hotter, more tenuous plasma.

5. Conclusions

On December 5th, 2004 the magnetosphere was being monitored by a constellation of spacecraft (including TC-1, TC-2 and Polar), providing a large-scale snapshot of the formation of the cold-dense plasma sheet (CDPS) which formed owing to sustained northward IMF during the passage of a coronal mass ejection (CME). This multi-spacecraft study allowed us to highlight the following features:

- The presence of a clear solar wind-originated LLBL at Polar, during a time interval when the occurrence of sub-solar reconnection was unlikely.
- The observation of quasi-continuous, high-latitude reconnection in both hemispheres, coupled with the lack of evidence of KH waves at Polar location, suggest that the LLBL observed by Polar is the result of double high-latitude reconnection, although other candidate processes cannot be completely ruled out.
- Flank boundary waves are observed by TC-1, which is located a few R_E tailward of Polar on the same side of the magnetosphere, and have typical properties (e.g., period) of the KH instability.

- These waves were confirmed to be unstable by running a KH MHD simulation using observed plasma parameters as inputs. This simulation also suggests reconnection could be facilitated by these waves.
- Further analysis of the density and velocity changes in this region suggests that the KH waves at TC-1 are 'rolled-up' and as such, that plasma transport is possibly occurring across the boundary.
- Electron phase space density comparisons, in addition to adiabatic consideration of flux transport, show that the LLBL at Polar is not sufficient to source the flank boundary layer observed at TC-1.
- It is thus envisaged that the KH instability also contributes to the formation of the boundary layers and CDPS on that day.
- The persistence of CDPS and BL plasma after ~18:00 UT suggests plasma transfer is not constrained to periods of strongly northward IMF.
- Thus, in essence, this study provides evidence of the simultaneous occurrence, and probable solar wind plasma penetration, owing to both dusk flank magnetopause KH wave activity and continuous high-latitude reconnection in both hemispheres.

Recent data from the Polar, TC-1, TC-2 and Cluster missions will provide us with more opportunities to investigate local time separated regions in the magnetosphere (due to evolution of the spacecraft orbits relative to one another). We hope such situations will enable us to ascertain the role (quantitatively) of each mechanism.

Acknowledgements

The authors would like to acknowledge the editor and reviewers of this manuscript for their patience and pertinent and helpful suggestions. We thank the International Space Science Institute in Bern, Switzerland, in particular B. Fasler, S. Saliba and V. Manno, for supporting the 'Comparative Cluster-Double Star Measurements of the Dayside Magnetosphere' team from which this work was developed. MGGTT would also like to thank M. Fujimoto and H. Hasegawa for useful discussions. ACE data was provided via CDAweb. We thank C.T. Russell and X. Liu for provision of MFE magnetometer data from Polar. Work at Los Alamos was performed under the auspices of the US Department of Energy, with support from NASA programs (Guest investigator and Living With a Star TR&T).

References

Carr, C., Brown, P., Zhang, T.L., Gloag, J., Horbury, T., Lucek, E., Magnes, W., O'Brien, H., Oddy, T., Auster, U., Austin, P., Aydogar, O., Balogh, A., Baumjohann, W., Beek, T., Eichelberger, H., Fornacon, K.-H., Georgescu, E., Glassmeier, K.-H., Ludlam, M., Nakamura, R., Richter, I. The Double Star Magnetic field investigation: instrument design, performance and highlights of the first year's observations, Ann. Geophys., SRef-ID: 1432-0576/ag/2005-23-2713, 2713–2732, 2005.

Chandler, M.O., Fuselier, S.A., Lockwood, M., Moore, T.E. Evidence of component merging equatorward of the cusp. J. Geophys. Res. 104 (22), 623–622, 633, 1999.

Domingo, V., Fleck, B., Poland, A.I. The SOHO mission: an overview, in: Fleck, B., Domingo, V., Poland, A.I. (Eds.), The SOHO Mission. Kluwer Academic Publishers, 1995.

Dungey, J.W. Interplanetary magnetic field and auroral zones. Phys. Rev. Lett. 6, 47, 1961.

Fairfield, D.H., Otto, A., Mukai, T., Kokubun, S., Lepping, R.P., Steinberg, J.T., Lazarus, A.J., Yamamoto, T. Geotail observations of the Kelvin–Helmholtz instability at the equatorial magnetotail boundary for parallel northward fields. J. Geophys. Res. 105 (A9), 21159–21173, 2000.

Fazakerley, A.N., Carter, P.J., Watson, G., Spencer, A., Sun, Y.Q., Coker, J., Coker, P., Kataria, D.O., Fontaine, D., Liu, Z.X., Gilbert, L., He, L., Lahiff, A.D., Mihaljcic, B., Szita, S., Taylor, M.G.G.T., Wilson, R.J., Dedieu, M., Schwartz, S.J. The Double Star Plasma Electron and Current Experiment. Ann. Geophys., SRef-ID: 1432-0576/ag/2005-23-2733, 2733–2756, 2005.

Fedder, J.A., Lyon, J.G. The Earth's magnetosphere is 165 R_E long: Self-consistent current, convection, *n* mangetospheric structure, and processes for northward interplanetary magnetic field. J. Geophys. Res. 100 (A3), 3623–3635, 1995.

Frey, H.U., Mende, S.B., Immel, T.J., Fuselier, S.A., Claflin, E.S., Gérard, J.-C., Hubert, B. Proton Aurora in the cusp. J. Geophys. Res. 107 (A7), 1091, doi:10.1029/2001JA900161, 2002.

Fujimoto, M., Teresawa, T. Anomalous ion mixing within an MHD scale Kelvin–Helmholtz vortex, 2. Effects of inhomogeneity. J. Geophys. Res. 100, 12,025, 1995.

Gosling, J.T., Thomsen, M.F., Bame, S.J., Onsager, T.G., Russell, C.T. The electron edge of the low-latitude boundary layer during accelerated flow events. Geophys. Res. Lett 17, 1833–1836, 1990.

Greenwald, R.A., Baker, K.B., Dudeney, J.R., Pinnock, M., Jones, T.B., Thomas, E.C., Villain, J.-P., Cerisier, J.-C., Senior, C., Hanuise, C., Hunsucker, R.D., Sofko, G., Koehler, J., Nielsen, E., Pellinen, R., Walker, A.D.M., Sato, N., Yamagishi, H. DARN/SuperDARN: a global view of the dynamics of high-latitude convection. Space Sci. Rev. 71, 761–796, 1995.

Harvey, P., Mozer, F.S., Pankow, D., Wygant, J., Maynard, N.C., Singer, H., Sullivan, W., Anderson, P.B., Pfaff, R., Aggson, T., Pederson, A., Fälthammar, C.-G., Tanskannen, P. The electric field instrument on the polar satellite. Space Sci. Rev. 71, 583–596, 1995.

Hasegawa, H., Fujimoto, M., Phan, T.-D., Rème, H., Balogh, A., Dunlop, M.W., Hashimoto, C., TanDokoro, R. Transport of solar wind into Earth's magnetosphere through rolled-up Kelvin–Helmholtz vortices. Nature 430, 755, 2004.

Hasegawa, H., Fujimoto, M., Takagi, K., Saito, Y., Mukai, T., Rème, H. Single Spacecraft detection of rolled-up Kelvin–Helmholtz vortices at the flank magnetoapuse. J. Geophys. Res. 111, A09203, doi:10.1029/2006JA011728, 2006.

Imber, S.M., Milan, S.E., Hubert, B. The auroral and ionospheric flow signatures of dual lobe reconnection. Ann. Geophys. 24, 3115–3129, 2006.

Johnson, J.R., Cheng, C.Z., Song, P. Signatures of mode conversion and kinetic alfven waves at the magnetopause. Geophys. Res. Lett. 28 (2), 227–230, 2001.

Kessell, R.L., Chen, S.-H., Green, J.L., Fung, S.F., Boardsen, S.A., Tan, L.C., Eastman, T.E., Craven, J.D., Frank, L.A. Evidence of high-latitude reconnection during northward IMF: Hawkeye observations. Geophys. Res. Lett. 23, 583–586, 1996.

Lavraud, B., Dunlop, M.W., Phan, T.D., Rème, H., Bosqued, J.-M., Dandouras, I., Sauvaud, J.-A., Lundin, R., Taylor, M.G.G.T., Cargill, P.J., Mazelle, C., Escoubet, C.P., Carlson, C.W., McFadden, J.P., Parks, G.K., Moebius, E., Kistler, L.M., Bavassano-Cattaneo, M.-B., Korth, A., Klecker, B., Balogh, A. Cluster observations of the exterior cusp and its surrounding boundaries under northward IMF. Geophys. Res. Lett. 29 (20), doi:10.1029/2002GL015464, 2002.

Lavraud, B., Thomsen, M.F., Taylor, M.G.G.T., Wang, Y.L., Phan, T.-D., Schwartz, S.J., Elphic, R.C., Fazakerley, A., Reme, H., Balogh, A. Characteristics of the magnetosheath electron boundary layer under northward interplanetary magnetic field: Implications for high-latitude reconnection. J. Geophys. Res. 110, A06209, doi:10.1029/2004JA010808, 2005.

Lavraud, B., Thomsen, M.F., Lefebvre, B., Schwartz, S.J., Seki, K., Phan, T.D., Wang, Y.L., Fazakerley, A., Rème, H., Balogh, A. Evidence for newly closed magnetosheath field lines at the dayside magnetopause under northward IMF. J. Geophys. Res. 111, A05211, doi:10.1029/2005JA011266, 2006.

Li, W., Raeder, J., Dorelli, J., Øieroset, M., Phan, T.D. Plasma sheet formation during long period of northward IMF. Geophys. Res. Lett. 32, doi:10.1029/2004GL021523, 2005.

McComas, D.J., Bame, S.J., Barker, P., Feldman, W.C., Phillips, J.L., Riley, P., Griffee, J.W. Solar wind electron proton monitor (SWE-PAM) for the advanced composition explorer. Space Sci. Rev. 86, 563–612, 1998.

Mende, S.B., Heetderks, H., Frey, H.U., Lampton, M., Geller, S.P., Habraken, S., Renotte, E., Jamar, C., Rochus, P., Spann, J., Fuselier, S.A., Gerard, J.-C., Gladstone, R., Murphree, S., Cogger, L. Far ultraviolet imaging from the IMAGE spacecraft. 1. System design. Space Sci. Rev. 91 (1–2), 243–270, 2000.

Milan, S.E., Lester, M., Cowley, S.W.H., Brittnacher, M. Dayside convection and auroral morphology during an interval of northward interplanetary magnetic field. Ann. Geophys. 18, 436–444, 2000.

Nakamura, T.K.M., Fujimoto, M., Otto, A. Magnetic reconnection induced by weak Kelvin–Helmholtz instability and the formation of the low-latitude boundary layer. Geophys. Res. Lett. 33, L14106, doi:10.1029/2006GL026318, 2006.

Nykyri, K., Otto, A. Plasma transport at the magnetospheric boundary due to reconnection in Kelvin–Helmholtz vortices. Geophys. Res. Lett 28 (18), 3565–3568, 2001.

Nykyri, K. Influence of the Kelvin–Helmholtz Instability on the plasma transport at the magnetospheric boundary. PhD Thesis, 2002.

Nykyri, K., Otto, A., Lavraud, B., Mouikis, C., Kistler, L.M., Balogh, A., Rème, H. Cluster observation of reconnection due to the Kelvin–Helmholtz instability at the dawnside magnetosphere. Plasma transport at the magnetospheric boundary due to reconnection in Kelvin–Helmholtz vortices. Ann. Geophys. 24, 2619–2643, 2006.

Øieroset, M., Raeder, J., Phan, T.-D., Wing, S., McFadden, J.P., Li, W., Fujimoto, M., Reme, H., Balogh, A. Global cooling and densification of the plasma sheet during an extended period of purely northward IMF on October 22–24, 2003, Geophysical Research Letters, Vol. 32, doi:10.1029/2004GL021523, 2005.

Ogino, T., Walker, R.J., Abshourabdall, M. A global magnetohydrodynamic simulation of the response of the magnetosphere to a northward turning of the interplanetary magnetic field. J. Geophys. Res. 99 (A6), 11,027–11,042, 1994.

Onsager, T.G., Scudder, J.D., Lockwood, M., Russell, C.T. Reconnection at the high-latitude magnetopause during northward interplanetary magnetic field conditions. J. Geophys. Res. 106 (A11), 25,467–25,488, 2001.

Otto, A., Fairfield, D.H. Kelvin–Helmholtz instability at the magnetotail boundary: MHD simulation and comparison with geotail observations. J. Geophys. Res. 105, 21,175, 2000.

Phan, T.D., Larson, D., McFadden, J., Lin, R.P., Carlson, C., Moyer, M., Paularena, K.I., McCarthy, M., Parks, G.K., Reme, H., Sanderson, T.R., Lepping, R.P. Low-Latitude dusk flank magnetosheath, magnetopause and boundary layer for low magnetic shear: wind observations. J. Geophys. Res. 102, 19,883, 1997.

Raeder, J., Walker, R.J., Ashour-Abdalla, M. The Structure of the distant geomagnetic tail during long periods of northward IMF. Geophys. Res. Lett. 22, 349, 1995.

Raeder, J., Berchem, J., Ashour-Abdalla, M., Frank, L.A., Paterson, W.R., Ackerson, K.L., Kokubun, S., Yamamoto, T., Slavin, J.A. Boundary layer formation in the magnetotail: geotail observation and comparisons with global MHD simulations. Geophys. Res. Lett. 24, 951, 1997.

Rème, H., Dandouras, I., Aoustin, C., Bosqued, J.M., Sauvaud, J.A., Vallat, C., Escoubet, P., Cao, J.B., Shi, J., Bavassano-Cattaneo, M.B., Parks, G.K., Carlson, C.W., Pu, Z., Klecker, B., Moebius, E., Kistler, L., Korth, A., Lundin, R., and the HIA team, The HIA instrument onboard the Tan Ce 1 Double Star near-equatorial spacecraft and its first results. Ann. Geophys., SRef-ID: 1432-0576/ag/2005-23-2757, 2757–2774, 2005.

Runohoniemi, J.M., Baker, K.B. Large –scale imaging of high latitude convection with Super Dual Auroral Radar Network HF radar observations. J. Geophys. Res. 103, 20797–22081, 1998.

Russell, C.T., Snare, R.C., Means, J.D., Pierce, D., Dearborn, D., Larson, M., Barr, G., Le, G. 'The GGS Polar magnetic fields investigation. Space Sci. Rev. 71, 563–582, 1995.

Scholer, M., Treumann, R.A. The low-latitude boundary layer at the flanks of the magnetopause. Space Sci. Rev. 80, 341, 1997.

Scudder, J., Hunsacker, F., Miller, G., Lobell, J., Zawistowski, T., Ogilvie, K., Keller, J., Chornay, D., Herrero, F., Fitzenreiter, R., Fairfield, D., Needell, J., Bodet, D., Googins, J., Kletzing, C., Torbert, R., Vandiver, J., Bentley, R., Fillius, W., McIlwain, C., Whipple, E., Korth, A. Hydra, a 3-dimensional electron and ion hot plasma instrument for the Polar spacecraft of the GGS mission. Space Sci. Rev. 71, 459, 1995.

Smith, C.W., Acuna, M.H., Burlaga, L.F., L'Heureux, J., Ness, N.F., Scheifele, J. The ACE magnetic field experiement. Space Sci. Rev. 86, 613–632, 1998.

Song, P., Russell, C.T. A model of the formation of the low-latitude boundary layer. J. Geophys. Res. 97, 1411, 1992.

Stone, E.C., Frandsen, A.M., Mewaldt, R.A., Christian, E.R., Margolies, D., Ormes, J.F., Snow, F. The advanced composition explorer. Space Sci. Rev. 86 (1–4), 1–22, 1998.

Takagi, K., Hashimoto, C., Hasegawa, H., Fujimoto, M., TanDokoro, R. Kelvin–Helmholtz instability in a magnetotail flank-like geometry: three-dimensional MHD simulations. J. Geophys. Res. 11, A08202, doi:10.1029/2006JA011631, 2006.

Teresawa, T., Fujimoto, M., Mukai, T., Shinohara, I., Saito, Y., Yamamoto, T., Machida, S., Kokubun, S., Lazarus, A.J., Steinberg, J.T., Lepping, R.P. Solar wind control of density and temperature in the near-Earth plasma sheet: WIND/GEOTAIL collaboration. Geophys. Res. Lett. 24, 935, 1997.

Trattner, K.J., Fuselier, S.A., Petrinec, S.M. Location of the reconnection line for Northward interplanetary magnetic field. J. Geophys. Res. 109, A03219, doi:10.1029/2003JA009975, 2004.

Truemann, R.A., LaBelle, J., Bauer, T. Diffusion processes: an observational perspective, in: Song, P., Sonnerup, B., Thomsen, M. (Eds.), Physics of the Magnetopause, Geophys. Monit., Vol. 90. AGU, p. 331, 1995.

Tsyganenko, N.A., Stern, D.P. Modeling the global magnetic field of the large-scale Birkeland current system. J. Geophys. Res. 101, 27187–27198, 1996.

Wing, S., Newell, P.T. Central plasma sheet ion properties as inferred from ionospheric observations. J. Geophys. Res. 103, 6785, 1998.